

Local versus global electronic properties of chalcopyrite alloys: X-ray absorption spectroscopy and ab initio calculations

Rafael Sarmiento-Perez, Silvana Botti, C. S. Schnohr, I. Lauermann, A. Rubio, B. Johnson

► **To cite this version:**

Rafael Sarmiento-Perez, Silvana Botti, C. S. Schnohr, I. Lauermann, A. Rubio, et al.. Local versus global electronic properties of chalcopyrite alloys: X-ray absorption spectroscopy and ab initio calculations. *Journal of Applied Physics*, American Institute of Physics, 2014, 116, pp.093703. 10.1063/1.4893579 . hal-02309418

HAL Id: hal-02309418

<https://hal-univ-lyon1.archives-ouvertes.fr/hal-02309418>

Submitted on 4 Feb 2021

HAL is a multi-disciplinary open access archive for the deposit and dissemination of scientific research documents, whether they are published or not. The documents may come from teaching and research institutions in France or abroad, or from public or private research centers.

L'archive ouverte pluridisciplinaire **HAL**, est destinée au dépôt et à la diffusion de documents scientifiques de niveau recherche, publiés ou non, émanant des établissements d'enseignement et de recherche français ou étrangers, des laboratoires publics ou privés.

Local versus global electronic properties of chalcopyrite alloys: X-ray absorption spectroscopy and ab initio calculations

Rafael Sarmiento-Pérez, Silvana Botti, Claudia S. Schnohr, Iver Lauermann, Angel Rubio, and Benjamin Johnson

Citation: *Journal of Applied Physics* **116**, 093703 (2014); doi: 10.1063/1.4893579

View online: <http://dx.doi.org/10.1063/1.4893579>

View Table of Contents: <http://scitation.aip.org/content/aip/journal/jap/116/9?ver=pdfcov>

Published by the [AIP Publishing](#)

Articles you may be interested in

[Phase diagram of the CuInSe₂-CuGaSe₂ pseudobinary system studied by combined ab initio density functional theory and thermodynamic calculation](#)

J. Appl. Phys. **116**, 053512 (2014); 10.1063/1.4891829

[The structure of Mn-doped tris\(8-hydroxyquinoline\)gallium by extended x-ray absorption fine structure spectroscopy and first principles calculations](#)

J. Appl. Phys. **112**, 113519 (2012); 10.1063/1.4768841

[Hard x-ray photoelectron spectroscopy of chalcopyrite solar cell components](#)

Appl. Phys. Lett. **100**, 092108 (2012); 10.1063/1.3687197

[Ab initio elasticity of chalcopyrites](#)

J. Appl. Phys. **93**, 3789 (2003); 10.1063/1.1556179

[Ab initio near edge soft x-ray absorption fine structure \(Al-NEXAFS\) spectrum of ethylene](#)

J. Chem. Phys. **111**, 10537 (1999); 10.1063/1.480436



Instruments for Advanced Science

 <p>Gas Analysis</p> <ul style="list-style-type: none">dynamic measurement of reaction gas streamscatalysis and thermal analysismolecular beam studiesdissolved species probesfermentation, environmental and ecological studies	 <p>Surface Science</p> <ul style="list-style-type: none">UHV TPDSIMSend point detection in ion beam etchelemental imaging - surface mapping	 <p>Plasma Diagnostics</p> <ul style="list-style-type: none">plasma source characterizationetch and deposition process reactionkinetic studiesanalysis of neutral and radical species	 <p>Vacuum Analysis</p> <ul style="list-style-type: none">partial pressure measurement and control of process gasesreactive sputter process controlvacuum diagnosticsvacuum coating process monitoring
--	---	---	---

Contact Hiden Analytical for further details:
W www.HidenAnalytical.com
E info@hiden.co.uk
CLICK TO VIEW our product catalogue

Local versus global electronic properties of chalcopyrite alloys: X-ray absorption spectroscopy and *ab initio* calculations

Rafael Sarmiento-Pérez,^{1,a)} Silvana Botti,^{1,a),b)} Claudia S. Schnohr,^{2,a),c)}
 Iver Lauermaann,^{3,a)} Angel Rubio,^{4,5,a)} and Benjamin Johnson^{5,a),d)}

¹Institut Lumière Matière and ETSF, UMR5306 Université Lyon 1-CNRS, Université de Lyon, F-69622 Villeurbanne Cedex, France

²Institut für Festkörperphysik, Friedrich-Schiller-Universität Jena, Max-Wien-Platz 1, 07743 Jena, Germany

³Helmholtz-Zentrum Berlin für Materialien und Energie, Hahn-Meitner Platz 1, 14109 Berlin, Germany

⁴Nano-Bio Spectroscopy Group and ETSF Scientific Development Centre, Departamento de Física de Materiales, Centro de Física de Materiales CSIC-MPC and DIPC, Universidad del País Vasco UPV/EHU, Avenida de Tolosa 72, E-20018 San Sebastián, Spain

⁵Fritz Haber Institute, Max Planck Society, Faradayweg 4-6, 14195 Berlin, Germany

(Received 19 March 2014; accepted 8 August 2014; published online 2 September 2014)

Element-specific unoccupied electronic states of Cu(In, Ga)S₂ were studied as a function of the In/Ga ratio by combining X-ray absorption spectroscopy with density functional theory calculations. The S absorption edge shifts with changing In/Ga ratio as expected from the variation of the band gap. In contrast, the cation edge positions are largely independent of composition despite the changing band gap. This unexpected behavior is well reproduced by our calculations and originates from the dependence of the electronic states on the local atomic environment. The changing band gap arises from a changing spatial average of these localized states with changing alloy composition. © 2014 AIP Publishing LLC. [<http://dx.doi.org/10.1063/1.4893579>]

I. INTRODUCTION

Photovoltaic conversion efficiencies of more than 20% have been demonstrated on both glass substrates and flexible polymer foils for Cu(In,Ga)Se₂ (CIGSe) based thin film solar cells.^{1,2} The properties of this absorber material can be tuned not only by adjusting the In to Ga ratio but also by substituting S for Se, obtaining Cu(In,Ga)(S,Se)₂ (CIGSSe) alloys, which is particularly interesting from an industrial point of view. Detailed knowledge of the relationship between material composition, structure, and electronic properties is therefore indispensable in order to exploit the full potential of these CIGSSe chalcopyrite systems for solar cell applications.

Regarding the pure sulfides, the band gap changes from ~1.5 eV for CuInS₂ (CIS) to ~2.4 eV for CuGaS₂ (CGS). This change is caused by a small shift of the valence band maximum and a much larger shift of the conduction band minimum. Unoccupied states can be accurately probed by near edge X-ray absorption fine structure (NEXAFS) spectroscopy, where an absorbed photon excites a core level electron into an empty conduction band state according to dipole transition rules. Therefore, the NEXAFS absorption signal contains information about the empty density of states of the material as well as transition probabilities. As we will show in this letter, however, the relationship between absorption edge position and conduction band minimum is far from trivial and depends sensitively on the local atomic environment.

II. X-RAY ABSORPTION SPECTROSCOPY

NEXAFS measurements were performed on bare solar cell grade CuIn_xGa_{1-x}S₂ (CIGS) thin-films, with $x = 0, 0.67,$ and 1. The samples were grown by rapid thermal processing and etched in KCN (see Ref. 3 for details). Figures 1 and 2 plot the S and Ga K-edge spectra, respectively. Because it is difficult to obtain an absolute energy scale for absorption measurements, the x-axes of the NEXAFS spectra remain in excitation (or photon) energy. The spectra from a single element in each figure have a common, although not necessarily absolute energy scale so that real shifts between the absorption edges can be considered. The shifts correspond to changing energetic differences between the initial and final states in the individual materials caused by an opening of the optical band gap. For a complete discussion of the NEXAFS measurements and considerations in analysis, see Ref. 3.

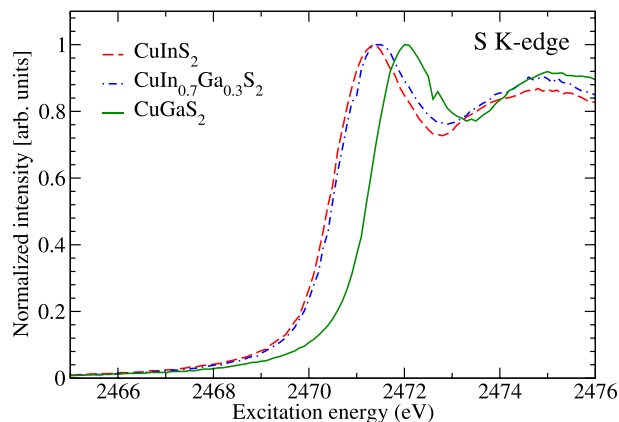


FIG. 1. Measured absorption K-edges of S in CuInS₂ (red dashed line), CuIn_{0.67}Ga_{0.33}S₂ (blue dotted-dashed line), and CuGaS₂ (green solid line).

^{a)}R. Sarmiento-Pérez, S. Botti, C. S. Schnohr, I. Lauermaann, A. Rubio, and B. Johnson made critical and independent contributions to this work.

^{b)}Electronic mail: silvana.botti@univ-lyon1.fr

^{c)}Electronic mail: c.schnohr@uni-jena.de

^{d)}Electronic mail: benjamin.johnson@alumni.tu-berlin.de

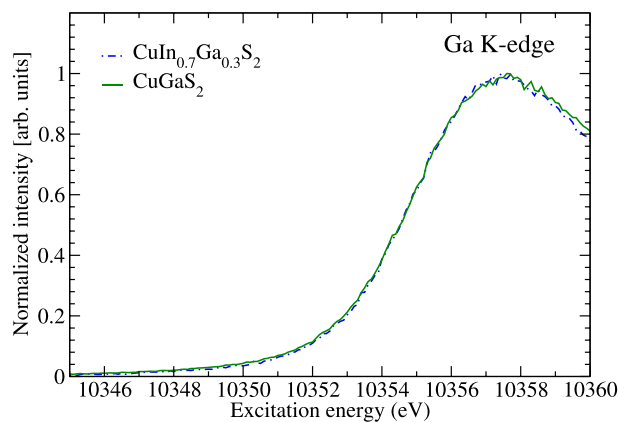


FIG. 2. Measured absorption K-edges of Ga in $\text{CuIn}_{0.67}\text{Ga}_{0.33}\text{S}_2$ (blue dotted-dashed line) and CuGaS_2 (green solid line).

As expected, the S K-edge position in Figure 1 shifts to higher energies when the Ga content of the material and thus the band gap is increased. In contrast, no change in edge position is observed for the Ga K-edge in Figure 2. The latter behavior is also observed for the Cu K-edge, the In and Ga L_3 -edges, and the In $M_{4,5}$ -edge, while the S L_3 -edge exhibits again a significant shift (see supplementary material⁴ and Ref. 3). This means that although the band gap and thus the energy of the conduction band minimum changes, only the anion absorption edges exhibit a corresponding shift supplying relevant macroscopic electronic information, whereas the cation absorption edges remain unchanged. X-ray absorption measurements of $\text{CuIn}_x\text{Ga}_{1-x}\text{Se}_2$ ($0 \leq x \leq 1$) also show no appreciable shift in the Cu, Ga, and In K-edge positions⁵ suggesting that these findings represent general features of material systems with different cation species such as, but not limited to, chalcopyrites. Note that a similar behaviour was in fact observed in the completely different context of the investigation of magnetism and insulator/metal transitions as a function of doping for Sr doped cobaltites ($\text{La}_{1-x}\text{Sr}_x\text{CoO}_3$).⁶ NEXFAS studies on these alloys show a very small Co K-edge shift with increasing x ,^{7,8} in contrast with large shifts observed in other Co systems, while extended x-ray absorption fine structure (EXAFS) results yield a Co-O bond length nearly independent of x .⁸ This points to a correlation between the electronic structure and the local atomic environment and thus to the need of a correct description of the latter⁶ as will be discussed in detail in Sec. IV for the case of mixed chalcopyrite semiconductors.

III. DENSITY FUNCTIONAL THEORY (DFT) CALCULATIONS

In order to unravel the origin of this unexpected behavior, we performed DFT calculations of the electronic states of $\text{CuIn}_x\text{Ga}_{1-x}\text{S}_2$ alloys, for $x=0, 0.3, 0.5, 0.7$, and 1. The projected partial densities of states (pDOS) exhibit the same dependence on or independence of the composition as the measured NEXAFS spectra. We explain this behavior in terms of the element-specific atomic-scale structure that determines the density of states and thus the electronic properties of the material.

We studied CIGS chalcopyrite alloys focusing on the composition dependence of the pDOS. Alloys were simulated by building special quasi-random structures (SQS),⁹ i.e., periodic N -atom supercells whose correlation functions are the best match to the ensemble averaged correlation functions of the random alloy. In the literature, a substitutional random alloy is very often represented through “non structural” approximations (such as the virtual crystal approximation or the site coherent potential approximation¹⁰), which consider only average occupations of the lattice sites and give no information dependent on the local arrangement of atoms. However, the electronic states of the CIGS compounds are known to be very sensitive to modifications of the internal structural parameters.^{11,12} This fact necessitates a proper description of the microscopic atomic structure of CIGS alloys, and it motivates our choice to work with supercells, despite the increased computational cost.

We built SQS of $\text{CuIn}_x\text{Ga}_{1-x}\text{S}_2$ for $x \simeq 1/3$, $x = 1/2$, and $x \simeq 2/3$ using the code ATAT.¹³ The SQS supercells contained 40, 54, or 64 atoms and they include all three possible environments for S: 2 Cu and 2 Ga neighbors, 2 Cu and 2 In neighbors, and 2 Cu, 1 Ga, and 1 In neighbors, as described in Ref. 5. We did not consider defects (e.g., cation antisites) so that all S atoms are surrounded by 2 Cu and 2 atoms of the group III, yielding always the same number of valence electrons. The supercells were relaxed using the all-electron projector augmented wave method as implemented in the code VASP.^{14,15} Brillouin zone integrals were converged with a 340 eV plane-wave cutoff and a $3 \times 3 \times 3$ shifted k-point mesh. We tested different exchange-correlation potentials: Perdew–Burke–Ernzerhof (PBE),^{16,17} PBE + U (Ref. 18) with $U = 6$ eV on Cu d states, and the screened hybrid Heyd–Scuseria–Ernzerhof (HSE).^{19,20} For the ternary materials, it is already known that anion–cation bond lengths are poorly estimated when using standard semi-local functionals (such as PBE),^{11,21,22} causing an underestimation of the band gap by more than 50% at the relaxed structure.¹¹ In the mixed cation systems, three cation species lead to three independent anion–cation bond lengths with two different displacement mechanisms.¹²

After relaxing all the SQS cells, we compared the geometries and the density of states of the supercells of different sizes corresponding to the same stoichiometry. We observed that SQS supercells with 40 atoms already give bond lengths that differ by less than 0.002 Å and density of states substantially identical to those of the 64 atom supercells. In view of that, all results shown in the following were obtained with the 40-atom SQS cells. A further validation of our model structures comes from the comparison with EXAFS measurements of CIGS alloys, which yield the element-specific atomic-scale structure, in particular, the Cu-S, Ga-S, and In-S distances.¹² The atomic positions obtained with the HSE functional always yield bond lengths in excellent agreement with experimental data (see Table 1 of the supplementary material⁴). In contrast, PBE and, to a smaller extent, PBE + U overestimates Ga-S and In-S bond lengths, while Cu-S bond lengths remain quite close to HSE and experimental values. However, all three bond lengths, Cu-S, Ga-S, and In-S, should be as close as possible to experimental

TABLE I. Calculated and measured valence band offsets ΔV_{BM} and band gaps E_{gap} of $\text{CuIn}_x\text{Ga}_{1-x}\text{S}_2$ alloys. Experimental values are from Ref. 3.

In/(In + Ga)	ΔV_{BM}		E_{gap}	
	HSE (eV)	exp	HSE (eV)	exp
0.0	0.00	0.0	2.20	2.4
0.3	0.06	...	1.90	...
0.5	0.10	...	1.69	...
0.7	0.11	0.3	1.55	1.6
1.0	0.14	0.3	1.32	1.5

values as their combination determines the anion displacement.¹² Our findings for alloy systems are thus consistent with previous results for the pure ternaries^{11,22} and demonstrate that the use of HSE is crucial to correctly reproduce the atomic-scale structure.

Besides giving the best structural parameters, HSE yields a band gap very close to the experimental value (see Table I).^{11,23} Therefore, it appears judicious to also consistently use HSE to calculate (partial) densities of states. In order to evaluate band offsets, it was necessary to align the band edges of compounds of different chemical compositions. For this, we used the method from Schleife *et al.*²⁴ and aligned the branch-point energies, defined as the energy at which the defect states induced in the gap change their character from predominantly acceptor-like to donor-like. Reaching from one material into another at the interface such states transfer a net charge, the sign of which depends on the position of the Fermi level relative to the branch point energy. This charge transfer leads to an intrinsic interface dipole that tends to line up the energy bands in a way that the dipole itself vanishes. Therefore, branch point energies are relevant reference levels for the band alignment, and their use allows us to avoid the direct calculations of interfaces.

Figures 3 and 4 plot the calculated pDOS of the S and Ga *p*-states, respectively, for the conduction bands of CIGS with varying composition. A Gaussian broadening of 0.3 eV is applied to all the calculated pDOS. According to the

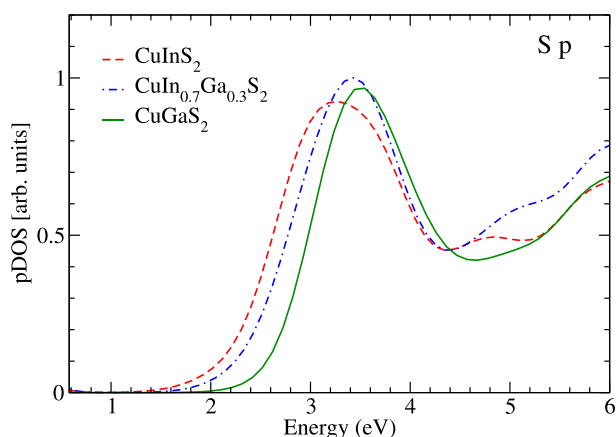


FIG. 3. Calculated pDOS of *p* states on S atoms for the conduction bands of CuInS_2 (red dashed line), $\text{CuIn}_{0.7}\text{Ga}_{0.3}\text{S}_2$ (blue dotted-dashed line), and CuGaS_2 (green solid line). The valence band maximum of CuInS_2 is set to zero and the energy scales of different compounds are aligned via the branch point energy.

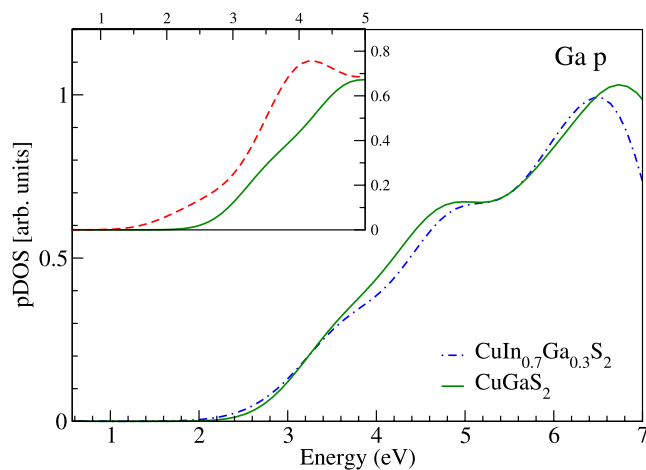


FIG. 4. Calculated pDOS of *p* states on Ga atoms for conduction bands of $\text{CuIn}_{0.7}\text{Ga}_{0.3}\text{S}_2$ (blue dotted-dashed line) and CuGaS_2 (green solid line). Inset: pDOS of Ga *p*-states in the conduction band for CGS with either CGS lattice constants (green solid line) or with average lattice constants between CIS and CGS (red dashed line).

dipole selection rules, electrons from the K-shell (*s* orbitals) are excited to unoccupied conduction band states with *p* character. Furthermore, transitions only take place if the final and initial states overlap in space.²⁵ Since the core level states, particularly of the K-shell, are highly localized at the absorbing atom, the electrons will be excited to those unoccupied states whose amplitudes dominate at the absorber site, namely the states of the absorbing atom itself. Thus, the pDOS of the S and Ga *p*-states corresponds to the unoccupied states sampled at the S and Ga K-edge as shown in Figures 1 and 2.

The comparison remains qualitative as the effects on the experimental absorption spectra from the core-hole created in the excitation process, such as many-body relaxation and core-hole lifetime broadening,^{25,26} are beyond the scope of our DFT calculation. The transition matrix elements which further influence the experimental absorption spectra are also not part of the calculation. Nevertheless, the qualitative agreement between calculated and measured pDOS is excellent as can be seen from comparing Figures 1 and 3 as well as Figures 2 and 4. In particular, a significant shift of the edge position with alloy composition is observed for S in both cases, whereas the Ga edge position remains unchanged for both experiment and calculation. Similar agreement is also obtained for the Cu K-edge, for the L_{3-} edges corresponding to unoccupied states with *s* and *d* character and for *p* and *f* states in the case of In- $M_{4,5}$ -edge (see supplementary material⁴). The case of the Cu L_{3-} edge is more ambiguous, as discussed in Ref. 3, and more experimental and theoretical research is required to draw reliable conclusions on the behavior at this edge. The theoretical findings thus confirm the experimental observations demonstrating that this unusual behavior of absorption edge positions is indeed a real effect of mixed chalcopyrite alloys.

IV. DISCUSSION

The fact that the Ga, In, and Cu absorption edge positions remain nearly unaltered with alloy composition despite

a significant change of the band gap closely resembles the fact that the element-specific Ga-S, In-S, and Cu-S bond lengths are nearly constant over the whole compositional range despite a significant change of the lattice constants.¹² In contrast, both the S edge position and the average group-III-S bond length vary with changing In/Ga ratio. This strongly suggests that the absorption edge position, i.e., the energy of the element-specific unoccupied local states, is determined by the local atomic arrangements rather than the overall crystallographic structure.

CIGS alloys crystallize in the chalcopyrite structure⁵ where each Ga, In, or Cu cation is bonded to four S anions. If all atoms occupied ideal lattice sites, the Ga-S and In-S bond lengths would be identical and would change with alloy composition according to the change in lattice constants. (Note that the Cu-S bond length is nearly the same for CGS and CIS and hence no significant structural change is expected for the alloy.) The local structural environment surrounding the Ga or In atoms would thus be expanded or compressed leading to a change in band gap according to the well-known dependence on pressure or temperature. Consequently, the absorption edge position would shift with varying alloy composition. This effect is illustrated in the inset of Figure 4 where the calculated pDOS of Ga *p*-states in the conduction band is plotted for CGS with either the real CGS lattice constants or with those applying to the $x=0.5$ alloy. The edge position clearly shifts as the Ga-S bond length is stretched from the ternary length to the distance of the alloy lattice sites.

Obviously, this does not correspond to the behavior of the real CIGS alloys as shown in Figures 2 and 4 with the reason being that the local atomic arrangements strongly deviate from the average crystallographic structure. EXAFS measurements of both CIGS and CIGSe have shown that the element-specific bond lengths are nearly constant over the whole compositional range despite the change in lattice constants.^{5,12} This behavior closely resembles the findings for other mixed semiconductor systems as first reported for (In,Ga)As (Ref. 27) and later confirmed for many other III-V and II-VI ternary compounds.^{28,29} It originates from the fact that bond bending is energetically favored over bond stretching such that the lattice mismatch is accommodated in the mixed system mostly by a change of the bond angles and only to a small extent by a change of the bond lengths.^{28,30} In mixed cation systems, this is achieved by a displacement of the anion from its ideal lattice site,³¹ which has been shown to influence the band gap of the material for both III-V alloys³² and mixed chalcopyrites.^{5,12} This demonstrates again the strong similarity between these tetrahedrally coordinated mixed semiconductors and highlights the correlation between atomic-scale structure and electronic properties. However, due to the increased complexity of the chalcopyrites compared to the III-V or II-VI compounds, two different displacement mechanisms must be distinguished for CIGS and CIGSe as discussed in detail in Refs. 5 and 12.

For understanding the behavior of the absorption edge positions discussed here, the important feature of the atomic-scale structure is the fact that the element-specific Ga-S, In-S, and Cu-S bond lengths remain close to the ternary values over the whole compositional range. As a consequence

of this bond length preservation, the local structural environment surrounding the Ga, In, or Cu atoms changes very little and the projected pDOS still resembles that of the pure ternary compounds. The corresponding absorption edge position is thus independent of the alloy composition and remains fixed at the ternary energy position.

In contrast, the S anions are bonded to two Cu and two group-III atoms which can be either Ga or In. Consequently, the average first nearest neighbor environment of S changes with changing alloy composition even if the element-specific bond lengths remain constant. The S pDOS in the alloy thus represents a weighted average of the S pDOS in CGS and CIS corresponding to an absorption edge position that shifts with changing In/Ga ratio as seen in Figures 1 and 3. The change of the band gap, i.e., the shift of the conduction band minimum, is thus caused by a changing spatial average over the element-specific local states rather than by a change in energy of these states themselves. As a consequence, a determination of the conduction band minimum and thus the band gap from X-ray absorption spectroscopy studies is not straightforward in semiconductor alloys and care has to be taken when evaluating such data.

A very similar behavior can be found in Yamazoe *et al.* where Cu-In-Se compounds were studied with different Cu/In ratios varying from 1 (CuInSe₂) to 0.2 (CuIn₅Se₈).³³ While the Cu and In K-edge NEXAFS are independent of the sample stoichiometry, the Se K-edge NEXAFS exhibits significant changes as the Cu/In ratio decreases. Despite the different crystal structures of the various compounds, the Cu and In cations are bonded to four Se anions the distance to which varies only little with stoichiometry. The local structural environment of Cu and In, and hence the pDOS, therefore, remains mostly unchanged. In contrast, the average surrounding of the Se anions changes strongly with changing Cu/In ratio as clearly evidenced by the changing NEXAFS spectra. In view of these similarities between CIGS and Cu-In-Se compounds and given the remarkable resemblance of the atomic-scale structure of CIGS and CIGSe,^{5,12} we strongly believe that the findings presented in this work are general features of tetrahedrally coordinated semiconductors with different cation species and varying composition or stoichiometry. The similarity between our study and those on La_{1-x}Sr_xCoO₃ already mentioned above⁶⁻⁸ further suggests that this behaviour is even more general and can be found whenever an alloy contains elements for which the local first nearest neighbor environment does or does not change with changing alloy composition. For both CIGS and La_{1-x}Sr_xCoO₃, the nature and distance of the anions surrounding the cations do not change and the cation absorption edge position does not shift. In contrast, the local environment surrounding the anions does change with alloy composition and consequently the anion absorption edge positions do shift in both cases.

V. CONCLUSION

In conclusion, NEXAFS measurements and DFT calculations of CIGS show that the absorption edge position for Ga, In, and Cu is independent of the composition, whereas

the S absorption edge shifts with changing In/Ga ratio in accordance with the change in bandgap. This behavior originates from the state selectivity of the absorption process in which the core level electron is excited predominantly into unoccupied states of the absorbing atom itself. These element-specific local states are determined by the atomic-scale structural environment, which is nearly independent of composition for the Ga, In, and Cu cations but varies significantly with changing In/Ga ratio for the S anions. The observed change in the band gap with changing alloy composition thus results from a changing spatial average of the nearly unchanged element-specific local states. This clearly demonstrates the strong influence of local structural parameters on the electronic properties of the material. For those to be predicted correctly, the DFT calculation therefore has to reproduce not only the crystallographic structure correctly but also the atomic-scale structural parameters such as element-specific bond lengths and anion displacement which necessitates the use of the HSE exchange-correlation potential. While the study was performed for the specific case of CIGS, we believe that our findings are also applicable to other compound semiconductors with different cation species and varying composition or stoichiometry.

ACKNOWLEDGMENTS

We thank to Dr. Antje Vollmer and Dr. Michela Gorgoi for experimental help at the Bessy Synchrotron. S.B. acknowledges financial support from the French ANR project ANR-12-BS04-0001-02. A.R. acknowledges financial support from the European Research Council Advanced Grant DY-Namo (ERC-2010-AdG-267374), Spanish Grant (FIS2010-21282-C02-01), and Grupos Consolidados UPV/EHU del Gobierno Vasco (IT-578-13). C.S.S. was supported by the Carl-Zeiss-Stiftung Germany and by the German Federal Ministry for Economic Affairs and Energy (comCIGS-II project, 0325448 E). Computational resources were provided by GENCI (project x2013096017). The collaboration was established through ETSF (user project n.424).

¹P. Jackson, D. Hariskos, E. Lotter, S. Paetel, R. Wuerz, R. Menner, W. Wischmann, and M. Powalla, *Prog. Photovoltaics* **19**, 894 (2011).

²A. Chirila, P. Reinhard, F. Pianezzi, P. Bloesch, A. R. Uhl, C. Fella, L. Kranz, D. Keller, C. Gretener, H. Hagendorfer, D. Jaeger, R. Erni, S. Nishiwaki, S. Buecheler, and A. N. Tiwari, *Nature Mater.* **12**, 1107 (2013).

³B. Johnson, J. Klaer, S. Merdes, M. Gorgoi, B. Höpfner, A. Vollmer, and I. Lauermann, *J. Electron Spectrosc.* **190**, 42 (2013).

⁴See supplementary material at <http://dx.doi.org/10.1063/1.4893579> for the measured and calculated spectra of the other absorption edges.

⁵C. S. Schnohr, H. Kämmer, C. Stephan, S. Schorr, T. Steinbach, and J. Rensberg, *Phys. Rev. B* **85**, 245204 (2012).

⁶S. Medling, Y. Lee, H. Zheng, J. F. Mitchell, J. W. Freeland, B. N. Harmon, and F. Bridges, *Phys. Rev. Lett.* **109**, 157204 (2012).

⁷T. Saitoh, T. Mizokawa, A. Fujimori, M. Abbate, Y. Takeda, and M. Takano, *Phys. Rev. B* **56**, 1290 (1997).

⁸Y. Jiang, F. Bridges, N. Sundaram, D. P. Belanger, I. E. Anderson, J. F. Mitchell, and H. Zheng, *Phys. Rev. B* **80**, 144423 (2009).

⁹A. Zunger, S.-H. Wei, L. Ferreira, and J. Bernard, *Phys. Rev. Lett.* **65**, 353 (1990).

¹⁰M. Jaros, *Rep. Prog. Phys.* **48**, 1091 (1985).

¹¹J. Vidal, S. Botti, P. Olsson, J.-F. Guillemoles, and L. Reining, *Phys. Rev. Lett.* **104**, 056401 (2010).

¹²S. Eckner, H. Kämmer, T. Steinbach, M. Gnauck, A. Johannes, C. Stephan, S. Schorr, and C. S. Schnohr, *Appl. Phys. Lett.* **103**, 081905 (2013).

¹³A. van de Walle, P. Tiwary, M. de Jong, D. Olmsted, M. Asta, A. Dick, D. Shin, Y. Wang, L.-Q. Chen, and Z.-K. Liu, *Calphad* **42**, 13 (2013).

¹⁴G. Kresse and J. Furthmüller, *Comput. Mater. Sci.* **6**, 15 (1996).

¹⁵G. Kresse and J. Furthmüller, *Phys. Rev. B* **54**, 11169 (1996).

¹⁶J. P. Perdew, K. Burke, and M. Ernzerhof, *Phys. Rev. Lett.* **77**, 3865 (1996).

¹⁷J. P. Perdew, K. Burke, and M. Ernzerhof, *Phys. Rev. Lett.* **78**, 1396(E) (1997).

¹⁸V. I. Anisimov, J. Zaanen, and O. K. Andersen, *Phys. Rev. B* **44**, 943 (1991).

¹⁹J. Heyd, G. E. Scuseria, and M. Ernzerhof, *J. Chem. Phys.* **118**, 8207 (2003).

²⁰J. Heyd, G. E. Scuseria, and M. Ernzerhof, *J. Chem. Phys.* **124**, 219906(E) (2006).

²¹S. Botti, D. Kammerlander, and M. A. L. Marques, *Appl. Phys. Lett.* **98**, 241915 (2011).

²²I. Aguilera, J. Vidal, P. Wahnón, L. Reining, and S. Botti, *Phys. Rev. B* **84**, 085145 (2011).

²³L. Gütay, D. Regesch, J. K. Larsen, Y. Aida, V. Depredurand, A. Redinger, S. Caneva, S. Schorr, C. Stephan, J. Vidal, S. Botti, and S. Siebentritt, *Phys. Rev. B* **86**, 045216 (2012).

²⁴A. Schleife, F. Fuchs, C. Rödl, J. Furthmüller, and F. Bechstedt, *Appl. Phys. Lett.* **94**, 012104 (2009).

²⁵G. Bunker, *Introduction to XAFS* (Cambridge University Press, 2010).

²⁶J. J. Rehr and A. L. Ankudinov, *Coord. Chem. Rev.* **249**, 131 (2005).

²⁷J. C. Mikkelsen and J. B. Boyce, *Phys. Rev. Lett.* **49**, 1412 (1982).

²⁸C. S. Schnohr, L. L. Araujo, P. Kluth, D. J. Sprouster, G. J. Foran, and M. C. Ridgway, *Phys. Rev. B* **78**, 115201 (2008).

²⁹C. S. Schnohr, "Binary and ternary random alloys," in *X-ray Absorption Spectroscopy of Semiconductors*, edited by C. S. Schnohr and M. C. Ridgway (Springer, in press).

³⁰C. S. Schnohr, P. Kluth, L. L. Araujo, D. J. Sprouster, A. P. Byrne, G. J. Foran, and M. C. Ridgway, *Phys. Rev. B* **79**, 195203 (2009).

³¹A. Balzarotti, N. Motta, A. Kisiel, M. Zinnal-Starnawska, M. T. Czyzyk, and M. Podgórný, *Phys. Rev. B* **31**, 7526 (1985).

³²C. S. Schnohr, *J. Phys.: Condens. Matter* **24**, 325802 (2012).

³³S. Yamazoe, H. Kou, and T. Wada, *J. Mater. Res.* **26**, 1504 (2011).